

11-19-2010

Role of alpha 7 Nicotinic Acetylcholine Receptor in Calcium Signaling Induced by Prion Protein Interaction with Stress-inducible Protein 1

Flavio H. Beraldo
Western University

Camila P. Arantes
Ludwig Institute for Cancer Research; Universidade de Sao Paulo

Tiago G. Santos
Ludwig Institute for Cancer Research; A.C. Camargo Cancer Center

Nicolle G. T. Queiroz
Ludwig Institute for Cancer Research; A.C. Camargo Cancer Center

Kirk Young
Western University

See next page for additional authors

Follow this and additional works at: <https://ir.lib.uwo.ca/anatomypub>

 Part of the [Anatomy Commons](#), and the [Cell and Developmental Biology Commons](#)

Citation of this paper:

Beraldo, Flavio H.; Arantes, Camila P.; Santos, Tiago G.; Queiroz, Nicolle G. T.; Young, Kirk; Rylett, Jane R.; Markus, Regina P.; Prado, Marco A. M.; and Martins, Vilma R., "Role of alpha 7 Nicotinic Acetylcholine Receptor in Calcium Signaling Induced by Prion Protein Interaction with Stress-inducible Protein 1" (2010). *Anatomy and Cell Biology Publications*. 70.
<https://ir.lib.uwo.ca/anatomypub/70>

Authors

Flavio H. Beraldo, Camila P. Arantes, Tiago G. Santos, Nicolle G. T. Queiroz, Kirk Young, Jane R. Rylett, Regina P. Markus, Marco A. M. Prado, and Vilma R. Martins

Role of $\alpha 7$ Nicotinic Acetylcholine Receptor in Calcium Signaling Induced by Prion Protein Interaction with Stress-inducible Protein 1*

Received for publication, June 23, 2010, and in revised form, September 3, 2010. Published, JBC Papers in Press, September 13, 2010, DOI 10.1074/jbc.M110.157263

Flavio H. Beraldo^{†§}, Camila P. Arantes^{†¶}, Tiago G. Santos^{†||}, Nicolle G. T. Queiroz^{†||}, Kirk Young[§], R. Jane Rylett[§], Regina P. Markus^{**}, Marco A. M. Prado^{§††1}, and Vilma R. Martins^{†||2}

From the [†]Ludwig Institute for Cancer Research, Hospital Alemão Oswaldo Cruz, São Paulo 01323-903, Brazil, the [¶]Departamento de Bioquímica, Instituto de Química, Universidade de São Paulo, São Paulo 05508-900, Brazil, the ^{||}Centro de Tratamento e Pesquisa do Hospital AC Camargo, São Paulo 01508-010, Brazil, the [§]J. Allyn Taylor Centre for Cell Biology, Molecular Brain Research Group, Robarts Research Institute and Department of Physiology and Pharmacology, University Western Ontario, London, Ontario N6A 5K8, Canada, the ^{**}Departamento de Fisiologia, Instituto de Biociências, Universidade de São Paulo, São Paulo 05508-090, Brazil, and the ^{††}Department of Anatomy and Cell Biology, University Western Ontario, London, Ontario N6A 5K8, Canada

The prion protein (PrP^C) is a conserved glycosylphosphatidylinositol-anchored cell surface protein expressed by neurons and other cells. Stress-inducible protein 1 (STI1) binds PrP^C extracellularly, and this activated signaling complex promotes neuronal differentiation and neuroprotection via the extracellular signal-regulated kinase 1 and 2 (ERK1/2) and cAMP-dependent protein kinase 1 (PKA) pathways. However, the mechanism by which the PrP^C-STI1 interaction transduces extracellular signals to the intracellular environment is unknown. We found that in hippocampal neurons, STI1-PrP^C engagement induces an increase in intracellular Ca²⁺ levels. This effect was not detected in PrP^C-null neurons or wild-type neurons treated with an STI1 mutant unable to bind PrP^C. Using a best candidate approach to test for potential channels involved in Ca²⁺ influx evoked by STI1-PrP^C, we found that α -bungarotoxin, a specific inhibitor for $\alpha 7$ nicotinic acetylcholine receptor ($\alpha 7$ nAChR), was able to block PrP^C-STI1-mediated signaling, neuroprotection, and neuritogenesis. Importantly, when $\alpha 7$ nAChR was transfected into HEK 293 cells, it formed a functional complex with PrP^C and allowed reconstitution of signaling by PrP^C-STI1 interaction. These results indicate that STI1 can interact with the PrP^C- $\alpha 7$ nAChR complex to promote signaling and provide a novel potential target for modulation of the effects of prion protein in neurodegenerative diseases.

Prions are the infectious components of transmissible spongiform encephalopathies that can self-perpetuate by imprinting an anomalous conformation onto a glycosylphosphatidylinositol-anchored host protein known as the prion protein (PrP^C).³ Conversion of PrP^C to the protease-resistant prion is thought to be a major event in prion diseases (1). However, despite the wealth of knowledge on prions, the roles of PrP^C on synaptic function and neuronal health are still not completely understood. Studies in yeast, mammalian cells, and mouse models support the hypothesis that PrP^C plays a major role in neuroprotection and neuronal differentiation (for review, see Refs. 1–3).

In humans, the initial cognitive dysfunction observed in transmissible spongiform encephalopathies is remarkably similar to those observed in Alzheimer disease (AD). Therefore, synaptic failure is likely to play a major role in the cognitive alterations seen in these neurological disorders (4). For instance, in AD, the role for A β ligands in synaptic dysfunction has received considerable attention (5, 6). Interestingly, recent work provided evidence that PrP^C functions as a receptor for A β and that this interaction mediates some of the effects of A β oligomers in synaptic plasticity (7) although these results are controversial at the moment (8, 9). Moreover, PrP^C seems to regulate the β -secretase cleavage of amyloid precursor protein, thereby regulating the production of A β (10). In addition, α -secretase regulates the cleavage of PrP^C, generating an N-terminal fragment with neuroprotective activity (11, 12).

PrP^C also binds to transmembrane proteins such as the 67-kDa laminin receptor (13–15), neuronal cell adhesion molecule (16, 17), G protein-coupled serotonergic receptors (18), and low density lipoprotein receptor-related protein 1 (19, 20), which are able to promote intracellular signaling-mediated neuronal adhesion and differentiation as well as PrP^C internalization. Remarkably, PrP^C functions as a receptor or co-receptor for extracellular matrix proteins such as laminin (21, 22) and

* This work was supported by Fundação de Amparo à Pesquisa do Estado de São Paulo Grant 03-13189-2 and Programa Institutos Nacionais de Ciência e Tecnologia, do Conselho Nacional de Desenvolvimento Científico e Tecnológico (to V. R. M.). This work was also supported by grants from PrionNet-Canada (to M. A. M. P.) and Canadian Institutes for Health Research (to R. J. R. and M. A. M. P.) and fellowships from Fundação de Amparo à Pesquisa do Estado de São Paulo (to F. H. B., C. P. A., T. G. S., and N. G. T. Q.) and the Department of Foreign Affairs and International Trade-Canada (to F. H. B.).

¹ To whom correspondence may be addressed: Robarts Research Institute, University Western Ontario, P.O. Box 5015, 100 Perth Dr., London, ON N6A 5K8, Canada. Tel.: 519-663-5777 (ext. 24888); E-mail: mprado@robarts.ca.

² International Scholar of the Howard Hughes Medical Institute. To whom correspondence may be addressed: Ludwig Institute for Cancer Research, Rua João Julião 245 1A, São Paulo, SP 01323-903, Brazil. Tel.: 55-11-33883239; E-mail: vmartins@ludwig.org.br.

³ The abbreviations used are: PrP^C, prion protein; $\alpha 7$ nAChR, $\alpha 7$ nicotinic acetylcholine receptor; α Bgt, α -bungarotoxin; AD, Alzheimer disease; STI1, stress-inducible protein 1; THG, thapsigargin; VGCC, voltage-gated calcium channel.

vitronectin (23), as well as the secreted co-chaperone stress-inducible protein 1 (STI1) (24). These data suggest that glycosylphosphatidylinositol-anchored PrP^C is a potential scaffold receptor in a multiprotein, cell surface, signaling complex, that may be the basis for the multiple neuronal functions ascribed to PrP^C (2, 3, 25).

We demonstrated previously that PrP^C amino acids 113–128 constitute the STI1 binding site (24). Furthermore, PrP^C-STI1 engagement rescues retinal and hippocampal neurons from staurosporine-induced programmed cell death through activation of protein kinase A (PKA). Additionally, PrP^C-STI1 binding also induces the differentiation and protein synthesis in hippocampal neurons via extracellular signal-regulated kinase 1 and 2 (ERK1/2) and phosphoinositide 3-kinase (PI3K)–Akt–mTOR activation (26, 27). Trafficking of both PrP^C and STI1 following binding at the membrane regulates the ERK1/2 pathway, but does not alter PrP^C regulation of PKA signaling (28).

Although several signaling pathways triggered by PrP^C have been identified, little is known regarding how intracellular signaling is activated by PrP^C following its interaction with extracellular ligands. In this study we mapped the upstream signaling events triggered by PrP^C-STI1 binding to identify the putative transmembrane protein responsible for connecting this extracellular complex to the intracellular milieu. Our data show that hippocampal neuronal signaling induced by PrP^C-STI1 is dependent on calcium influx through the $\alpha 7$ nicotinic acetylcholine receptor ($\alpha 7$ nAChR). These results provide a novel mechanism by which PrP^C transduces extracellular signals, with implications for PrP^C-mediated regulation of synaptic function and neuronal differentiation.

EXPERIMENTAL PROCEDURES

Reagents—Mouse recombinant STI1 (His₆-STI1) and an STI1 deletion mutant lacking the PrP^C binding site (STI1 Δ 230–245) were purified as described previously (24). The mitogen-activated protein kinase MAPK/ERK1/2 (p44/p42 MAPK) inhibitor 1,4-diamino-2,3-dicyano-1,4-bis (2-aminophenylthio) butadiene (U0126) was purchased from Promega. The PKA inhibitor KT5720, phosphodiesterase inhibitor isobutylmethylxanthine, and 4'-6-diamidino-2-phenylindole (DAPI) were purchased from Calbiochem. The PKA activator (forskolin) was purchased from LC Laboratories (Woburn, MA). The L-type calcium channel blocker (nifedipine), Ca²⁺-ATPase inhibitor (thapsigargin, THG), FLAG beads, FLAG peptide, and anti-FLAG antibodies were obtained from Sigma-Aldrich. The Q-type Ca²⁺ channel blocker (ω -conotoxin MCVII) was purchased from Latoxan (Valence, France). The store-operated calcium channel blocker (SKF-96365) and $\alpha 7$ nAChR blocker (α -bungarotoxin, α Bgt) were purchased from Tocris Biociences (Ellisville, MO). Fluo-3 AM, neurobasal medium, Opti-MEM, Hanks' buffered saline solution, and Lipofectamine were obtained from Invitrogen. Anti-phospho-ERK1/2 and anti-total ERK1/2 antibodies were purchased from Cell Signaling Technology (Beverly, MA), and peroxidase-coupled goat anti-rabbit secondary antibody and enhanced chemiluminescence (ECL) solution were obtained from GE Healthcare. Complete Protease Inhibitor Mixture was purchased from Roche Applied Science. The PKA assay system kit was pur-

chased from Upstate Biotechnology. Anti-cleaved caspase-3, Alexa Fluor 488 anti-rabbit antibodies, and Alexa Fluor 647 α Bgt were purchased from Molecular Probes. Immu-Mount was purchased from Thermo Scientific (Waltham, MA). The monoclonal antibodies 3F4 and 6H4 against PrP^C were acquired from Abcam (Cambridge, MA) and Prionics (Schlieren, Switzerland).

Animals and Primary Neuronal Cultures—PrP^C-null mice (*Prnp*^{0/0}), descendants of the *Zrch1* line, were provided by Dr. Charles Weissmann (Scripps Florida). Wild-type animals were generated by crossing F1 descendants from 129/SV and C57BL/6J matings. All studies were conducted in accordance with National Institutes of Health guidelines for the care and use of animals and with animal protocols approved by the Institutional Animal Care and Use Committee.

Primary cultures of hippocampal neurons from embryonic day 17 (E17) wild-type (*Prnp*^{+/+}) or PrP^C-null mice (*Prnp*^{0/0}) were obtained as previously described (26) and plated onto poly-L-lysine (5 μ g/ml)-coated coverslips (35 mm) for 4 days.

Ca²⁺ Signaling and Data Analysis—Neurons and HEK 293 cells were loaded with 10 μ M intracellular Ca²⁺ indicator Fluo-3 AM for 30 min at 37 °C in the presence of neurobasal medium or Opti-MEM supplemented with 2 mM CaCl₂. Cells were washed three times with Hanks' buffered saline solution and resuspended in Krebs buffer (124 mM NaCl, 4 mM KCl, 25 mM Hepes, 1.2 mM MgSO₄, 10 mM glucose) supplemented with 2 mM CaCl₂. Ca²⁺-free experiments were performed in Krebs buffer without CaCl₂ plus 1 mM EGTA. Cells were preincubated (30 min) in the presence of 25 μ M SKF-96365, voltage-gated calcium channel (VGCC) inhibitors (1 μ M ω -conotoxin MCVII plus 50 μ M nifedipine) or 1 nM α Bgt. Cells were treated with recombinant STI1 (1 μ M for neurons and 2 μ M for HEK 293), which mimics the effects of STI1 secreted from astrocytes (28, 29). HEK 293 cells were also pretreated with monoclonal antibodies against PrP^C (6H4 and 3F4 both at 10 μ g/ml) followed by recombinant STI1 (2 μ M). In addition, recombinant STI1 deleted of the PrP^C binding site, STI1 Δ 230–245 (2 μ M) (26) was used in control experiments, and treatment with THG (1 μ M) was performed to estimate calcium responses. Data acquisition was performed by confocal microscope using either a Bio-Rad Radiance 2100/Nikon (TE2000U) or a Zeiss LSM 510 (Zeiss, Toronto, ON) with excitation at 488 nm (argon laser) and emission collected with bandpass filter at 522–535 nm. The fluorescence was normalized as F_1/F_0 (F_1 , maximal fluorescence after drug addition and F_0 , basal fluorescence before drug addition). Software-based analysis (WCIF ImageJ (National Institutes of Health)) allowed quantification of fluorescence imaging in selected cells as a function of time. Experiments were carried out with at least three different cell cultures, and 40–50 cells were monitored in each experiment. *Traces* represent typical single-cell responses.

ERK1/2 Activity—Primary hippocampal neurons (1×10^6 cells) from *Prnp*^{+/+} mice were plated on dishes pretreated with poly-L-lysine and stimulated with STI1 (350 nM) for 1 min (26) in the presence or absence of 2 mM CaCl₂. Some cells were also preincubated with 1 nM α Bgt for 30 min prior to STI1 treatment. Cells were rinsed with ice-cold phosphate-buffered saline (PBS) and lysed in Laemmli buffer. Cell extracts were

$\alpha 7$ Nicotinic Acetylcholine Receptor Activation by PrP^C

subjected to SDS-PAGE (10%), and proteins were transferred onto nitrocellulose membranes. The membranes were blocked (5% milk, 0.1% Tween 20 in Tris-buffered saline) for 1 h at room temperature, incubated with anti-phospho-ERK1/2 or anti-total ERK1/2 antibodies (1:2,000) overnight at 4 °C, followed by incubation with peroxidase-coupled, goat anti-rabbit secondary antibody (1:2,000) for 1 h at room temperature. Reactions were developed using ECL solution, and the bands obtained after x-ray film exposure to the membranes were analyzed by densitometric scanning and quantified using ImageJ software. Alternatively, in some experiments, a CCD-based system was used (Alpha Innotech). ERK1/2 band densities activity was quantified as a relative value representing the ratio between phospho-ERK1/2 and total ERK1/2 for each sample. Results represent five independent experiments for neurons and three separate experiments for HEK 293 cells.

PKA Activity—Primary hippocampal neurons (1×10^6 cells) were preincubated with 100 μM isobutylmethylxanthine for 1 h at 37 °C, followed by incubation with 1 μM STI1 in the presence or absence of extracellular CaCl_2 (2 mM) or forskolin (10 μM) for 20 min at 37 °C as a positive PKA signaling control. Cells were washed with cold PBS and homogenized in ice-cold extraction buffer (150 mM NaCl, 20 mM MgCl_2 , 1% Triton X-100, and 25 mM Tris-HCl, pH 7.4), including Complete Protease Inhibitor mixture. Cellular debris was removed by centrifugation at $6,000 \times g$ for 10 min. PKA activity was determined by [γ - ^{32}P]ATP incorporation to a PKA-specific substrate provided by the PKA assay system kit.

Neuritogenesis Assays—Primary hippocampal neurons (4×10^4) from wild-type (*Prnp*^{+/+}) mice were treated with STI1 (350 nM) and incubated for 24 h at 37 °C. Neuritogenesis mediated by STI1 was evaluated after preincubation with 10 nM αBgt for 30 min. The cells were fixed with 4% paraformaldehyde and 0.12 M sucrose in PBS, pH 7.4, for 20 min at room temperature, washed three times with PBS, and stained with hematoxylin.

Morphometric analyses were performed using ImageJ software and the Neuron J plug in. The parameters analyzed were percentage of cells with neurites and percentage of neurons with neurites longer than 30 μm , which represents three or more times the average cell body. Approximately 200 cells were analyzed per sample.

Cell Death Assay—Primary hippocampal cultures (7×10^4 cells) were treated with STI1 (1.2 μM) for 1 h, followed by staurosporine (50 nM) treatment for 16 h as described previously (26). Alternatively, αBgt (10 nM) was added to the cultures 30 min prior to incubation with STI1. Cells were then fixed with 4% paraformaldehyde and 0.12 M sucrose in PBS, pH 7.4, for 20 min, and immunofluorescence reactions were performed to detect cleaved caspase-3. Briefly, cells were permeabilized and blocked with PBS/0.2% Triton X-100 plus 5% BSA for 1 h and subsequently incubated with anti-cleaved caspase-3 primary antibody (1:200) diluted in PBS/0.2% Triton X-100 plus 1% BSA for 2 h. After rinsing with PBS, cells were incubated with Alexa Fluor 488 anti-rabbit antibody and DAPI for 1 h. Immunolabeled cells were imaged with a BX61 Olympus Fluorescence microscope. Cell death induced by staurosporine was addressed by counting the percentage of cleaved caspase-3-

positive cells. Results represent three independent experiments; at least 300 cells total were counted per condition.

DNA Constructs—The cDNA encoding the human $\alpha 7\text{nAChR}$ subunit was cloned from a human universal QUICK-Clone cDNA library (Clontech) using the forward primer, 5'-CGACAGCCGAGACGTGGA-3' and reverse primer, 5'-CCGATGGTACGGATGT GC-3', designed to prime from the untranslated regions of the sequence (NCBI Reference Sequence: NM_000746). A forward primer, introducing a BamHI restriction site and minimal Kozak sequence (5'-GCCGGGATCCGCCACCATGCGCTGCTCGCCGGGA-3') to the N terminus, and a reverse primer, introducing an XbaI restriction site, FLAG epitope tag sequence (DYKDDDDK) and stop codon (5'-CGGCTCTAGATTACTTGTCTGTCGTCGTCTTATAGTCCGCAAAGTTTTGGACACGGCC-3') to the C terminus, were used to clone the FLAG- $\alpha 7\text{nAChR}$ sequence into the pcDNA3.1 expression vector (Invitrogen).

The cDNA for human *resistance to inhibitors of cholinesterase 3* homolog (*Caenorhabditis elegans*) (hRIC3; NCBI Reference Sequence: NM_024557.2) was purchased from OriGene (Rockville, MD). A forward primer, introducing a KpnI restriction site and minimal Kozak sequence (5'-GGCGGTA-CCGCCACCATGGCGTACTCCACAGTGCAGAGAGTC-3') to the N terminus, and a reverse primer, introducing a NotI restriction site, HA epitope tag sequence (YPYDVPDYA) and stop codon (5'-GCGGCCGCCAACTCGCATAATCCCA-CATCATAACGGATACTCTAAACCCTGGGGGTTACGCTTCCT-3') to the C terminus, were used to clone the HA-hRIC3 sequence into the pcDNA5/FRT expression vector (Invitrogen).

HEK 293 Cell Transfection—Cells were transfected with plasmids expressing FLAG- $\alpha 7\text{nAChR}$ with or without those expressing HA-hRIC 3 (1:1), using either a modified calcium phosphate method (30, 31) or Lipofectamine. To test transfection efficiency, cells transferred to coverslips were incubated with 500 nM Alexa Fluor 647- αBgt in Hanks' buffered saline solution containing 0.1% BSA for 1 h on ice. For confocal microscopy analyses, cells were washed with Hanks' buffered saline solution, fixed with PLP (0.2% periodate, 1.4% lysine, 2% paraformaldehyde), and coverslips were mounted onto glass microscope slides with Immu-Mount. Images are single z-sections captured by an LSM 510 Meta laser scanning microscope with excitation at 633 nm (HeNe laser) and a 650–710-nm bandpass emission filter.

Co-immunoprecipitation Assays—HEK 293 cells were transfected with plasmids expressing mouse PrP^C bearing the 3F4 epitope (26) and FLAG- $\alpha 7\text{nAChR}$ with or without HA-RIC 3 (1:1) cDNAs, as described above. Two days after transfection, $2\text{--}3 \times 10^6$ cells were lysed in 250 ml of 50 mM Tris-HCl, pH 7.5, 150 mM NaCl, and 1% Triton X-100, plus protease inhibitors for 15 min on ice, followed by two sonication pulses. Protein extracts (800 μg) were incubated with 20 μl of FLAG beads for 16 h at 4 °C. Beads were washed three times with wash buffer (50 mM Tris-HCl, pH 7.5, 150 mM NaCl, pH 7.4, and proteins were eluted by incubating the beads with 15 μg of FLAG peptide (in 100 μl of 50 mM Tris-HCl, pH 7.4, and 150 mM NaCl) for 10 min at room temperature. One quarter of the eluate was resolved by 4–12% SDS-PAGE, followed by immunoblotting

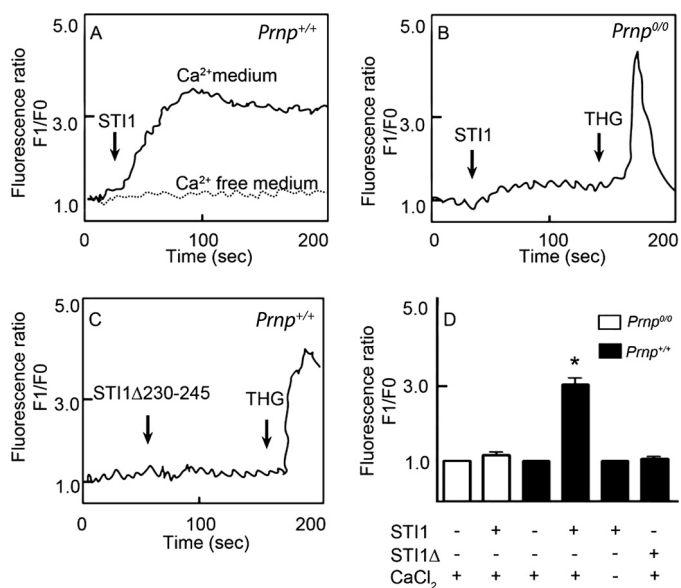


FIGURE 1. ST11 interaction with PrP^C promotes intracellular Ca²⁺ increase. *A* and *B*, Prnp^{+/+} (*A*) or Prnp^{0/0} (*B*) hippocampal neurons loaded with Fluo-3 AM were treated with ST11 (1 μM) in medium supplemented with (solid lines) or without (dashed line) Ca²⁺. THG-treated Prnp^{0/0} neurons show normal levels of intracellular Ca²⁺ stores. *C*, Prnp^{+/+} neurons were treated with an ST11 deletion mutant, ST11Δ230–245, lacking the PrP^C binding site. *D*, relative intracellular Ca²⁺ levels in Prnp^{0/0} (white bars) and Prnp^{+/+} (black bars) neurons treated with ST11 or ST11Δ230–245 in the presence or absence of CaCl₂ are indicated. The results represent the mean ± S.E. (error bars) of four independent experiments, and statistical significance was determined by one-way ANOVA and Newman-Keuls post test. *, *p* < 0.05 compared with controls.

with anti-FLAG antibodies. The remaining eluate was resolved with a second 4–12% SDS-PAGE, followed by immunoblotting with anti-PrP^C (3F4). These experiments were repeated four times.

Statistical Analysis—The statistical analyses were performed using GraphPad Prism 4. Results are represented as means ± S.E., and the total number of experiments is specified in each figure legend. Data were compared by one-way ANOVA and Newman-Keuls post test.

RESULTS

PrP^C-ST11 Interaction Increases Intracellular Ca²⁺—We demonstrated previously that PrP^C-ST11 engagement resulted in ERK1/2 phosphorylation and PKA activation, which in turn promoted neurogenesis and neuroprotection, respectively (26). Ca²⁺ signaling is an early event upstream of both PKA and ERK1/2 activation (32, 33). In addition, PrP^C has consistently been shown to modulate Ca²⁺ signaling (34–36). Therefore, to determine whether ST11 interaction with PrP^C affects intracellular Ca²⁺ levels, we performed Ca²⁺ imaging experiments on cultured hippocampal neurons using Fluo-3 AM. ST11 treatment promoted intracellular Ca²⁺ increases in neurons derived from Prnp^{+/+} mice (Fig. 1, *A* and *D*), but no effect was observed in neurons from Prnp^{0/0} mice (Fig. 1, *B* and *D*). However, treatment with THG, a blocker of the endoplasmic reticulum Ca²⁺-ATPase, mobilized the release of intracellular Ca²⁺ stores (Fig. 1*B*), suggesting that these stores were available in Prnp^{0/0} neurons. Consistent with these observations, intracellular Ca²⁺ levels remained unchanged in hippocampal neurons treated

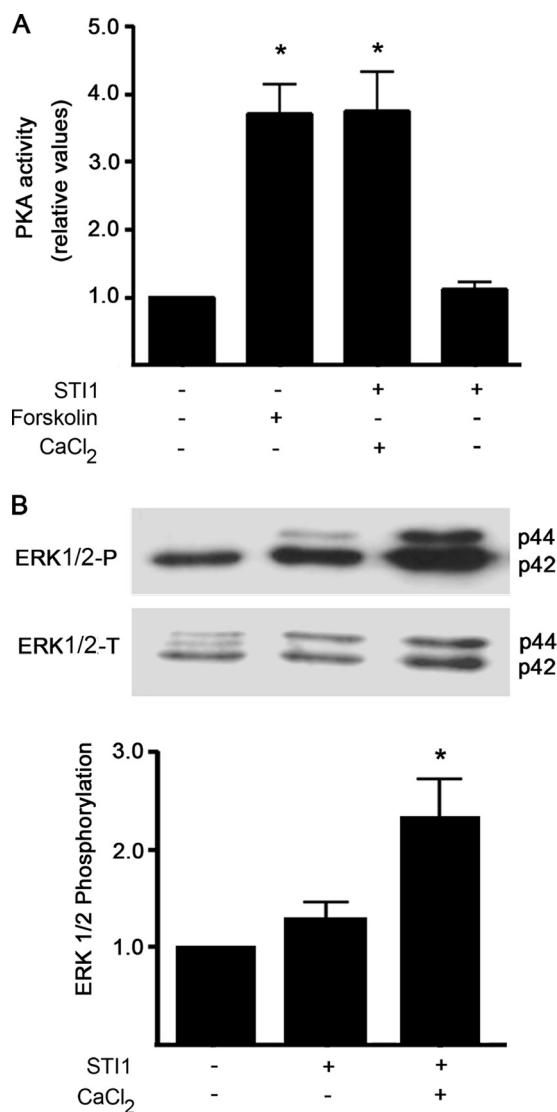


FIGURE 2. PKA activation and ERK1/2 phosphorylation are dependent on PrP^C-ST11-induced Ca²⁺ influx. PKA (*A*) and ERK1/2 (*B*) activation was induced by ST11 treatment in Prnp^{+/+} hippocampal neurons. Experiments were performed with or without CaCl₂, as indicated. Forskolin-treated cells were used as positive controls for PKA activation. Relative levels of ERK1/2 activity represent the ratio between phosphorylated ERK1/2 (upper panel) and total ERK1/2 (lower panel) normalized to the untreated group. The results represent the mean ± S.E. (error bars) of four independent experiments, and statistical significance was determined by one-way ANOVA and Newman-Keuls post test. *, *p* < 0.05 compared with controls.

with a mutant ST11 missing the PrP^C binding site (ST11Δ230–245) (Fig. 1, *C* and *D*). Interestingly, when Ca²⁺ was removed from the extracellular medium, ST11 had no effect on intracellular Ca²⁺ levels (Fig. 1, *A* and *D*). These results suggest that PrP^C-ST11 engagement can activate Ca²⁺ influx.

Ca²⁺ Influx Induced by PrP^C-ST11 Interaction Promotes ERK1/2 and PKA Activation—The effect of PrP^C-ST11-mediated Ca²⁺ influx on ERK1/2 and PKA activation was tested in wild-type neuronal cultures. In the presence of extracellular Ca²⁺, ST11 treatment increased both PKA and ERK1/2 activation (Fig. 2). Forskolin, which activates adenylyl cyclase and increases intracellular levels of cAMP, was used as a positive control for PKA activation (Fig. 2*A*). Conversely, no effect was observed when cells were treated with ST11 in the absence of

$\alpha 7$ Nicotinic Acetylcholine Receptor Activation by PrP^C

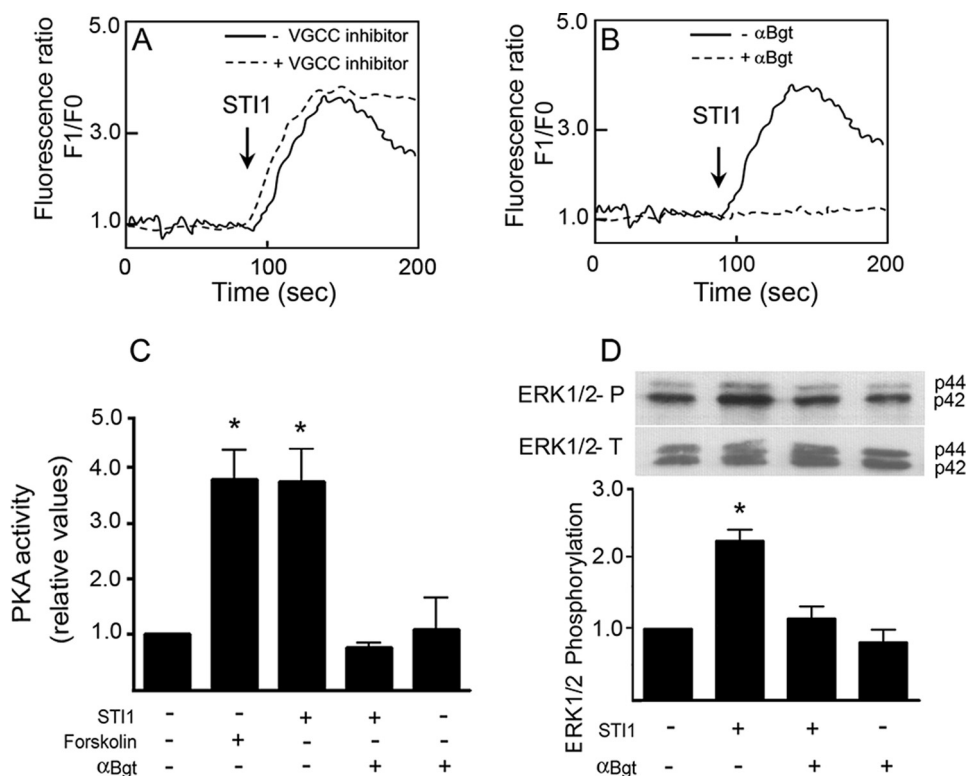


FIGURE 3. PrP^C-STII interaction induces Ca²⁺ influx, PKA and ERK1/2 activation through $\alpha 7$ nAChR. *A* and *B*, intracellular Ca²⁺ levels in *Prnp*^{+/+} hippocampal neurons were treated with STII (1 μ M) in the presence (dashed line) or absence (solid line) of VGCC inhibitors (*n* = 3) (*A*) or in the presence (dashed line) or absence (solid line) of α Bgt, a specific inhibitor of $\alpha 7$ nAChR (*n* = 4) (*B*). *C* and *D*, PKA activity (*n* = 3) (*C*) and ERK1/2 (*n* = 3) phosphorylation (*D*) were measured in *Prnp*^{+/+} hippocampal neurons treated with STII in the presence of α Bgt, as indicated. Forskolin was used as a positive control for PKA activation. Relative levels of ERK1/2 activity represent the ratio between phosphorylated ERK1/2 (upper panel) and total ERK1/2 (lower panel), normalized to the untreated group. The results were compared by one-way ANOVA and Newman-Keuls post test. *, *p* < 0.05 compared with controls.

extracellular Ca²⁺ (Fig. 2). Thus, upstream Ca²⁺ signaling is required for PrP^C-STII-mediated ERK1/2 and PKA activation.

PrP^C-STII Interaction Induces Ca²⁺ Influx through $\alpha 7$ nAChR—The PrP^C-STII interaction likely induces Ca²⁺ influx via modulation of an unidentified Ca²⁺ channel at the plasma membrane. Transmembrane Ca²⁺ channels include VGCCs and several ligand-gated channels. To determine the Ca²⁺ channel responsible for PrP^C-STII-mediated Ca²⁺ influx, we used a best candidate approach. To ascertain the role of VGCCs in this response, we used a VGCC inhibitor mixture (ω -conotoxin MCVIIC and nifedipine) targeting the majority of neuronal Ca²⁺ channels, including Ca_v2.1, Ca_v2.2, Ca_v1.1, Ca_v1.2, and Ca_v1.3. Hippocampal neurons still exhibited Ca²⁺ influx upon STII treatment in the presence of VGCC inhibitors (Fig. 3A), although Ca²⁺ influx due to KCl depolarization was blunted (data not shown).

To determine which ligand-gated channel might transduce PrP^C-STII-mediated Ca²⁺ influx, modulators of transient receptor potential channels and several neurotransmitter receptors (data not shown) were utilized. One candidate, the $\alpha 7$ nAChR, has been shown to activate PKA and ERK1/2 (37) and to promote neuronal differentiation and survival (38–40). In the presence of the $\alpha 7$ nAChR-specific inhibitor α Bgt, the PrP^C-STII-mediated intracellular Ca²⁺ influx was abolished (Fig. 3B). Moreover, PKA activation (Fig. 3C) and ERK1/2 phos-

phorylation (Fig. 3D) were completely blocked in the presence of α Bgt. These data show that STII binding to PrP^C induces intracellular Ca²⁺ influx via modulation of $\alpha 7$ nAChR, leading to ERK1/2 and PKA activation.

To verify whether $\alpha 7$ nAChR can be modulated by PrP^C-STII, we used HEK 293 cells, which do not express endogenous $\alpha 7$ nAChR, to reconstitute the expression of these receptors. HEK 293 cells were transfected with plasmid vectors encoding PrP^C, $\alpha 7$ nAChR, or $\alpha 7$ nAChR and RIC3 a chaperone that is required for correct assembly of this receptor at the cell surface (41). The functional expression of $\alpha 7$ nAChR at the cell surface was confirmed by binding of fluorescent α Bgt only upon its co-expression with RIC3 (Fig. 4A).

Co-immunoprecipitation experiments using anti-FLAG antibodies against FLAG-tagged $\alpha 7$ nAChR, followed by immunoblotting using anti-3F4 antibodies toward 3F4-tagged mouse PrP^C (28) or anti-FLAG antibodies, demonstrated that PrP^C physically interacts with $\alpha 7$ nAChR in these cells (Fig. 4B). To further test whether heterologous

expression of $\alpha 7$ nAChR was able to reconstitute PrP^C-STII-mediated Ca²⁺ signaling, we performed signaling experiments in HEK 293 cells. When these cells were transfected with empty vector (Fig. 5A), or with the vector encoding PrP^C alone (Fig. 5B), STII treatment did not induce an increase in the level of intracellular Ca²⁺. Similar results were observed in cells transfected only with $\alpha 7$ nAChR (Fig. 5C), likely due to the absence of RIC3. However, when HEK 293 cells were co-transfected with vectors encoding $\alpha 7$ nAChR, RIC3, and PrP^C, STII was able to increase intracellular Ca²⁺ (Fig. 5E). Interestingly, even in cells transfected only with $\alpha 7$ nAChR/RIC3, STII was able to evoke a Ca²⁺ signal although this effect could be blocked by antibodies against PrP^C (3F4 and 6H4) (Fig. 5D). In addition, STII deleted of the PrP^C binding site (STII Δ 230–245) was unable to induce Ca²⁺ signaling (Fig. 5F). These results indicate that endogenous levels of PrP^C expression in HEK 293 cells are sufficient to promote Ca²⁺ signaling when $\alpha 7$ nAChR is present. These data are quantified in Fig. 5G.

PrP^C-STII Interaction Induces PKA and ERK1/2 Activation through $\alpha 7$ nAChR—We also found that STII induced both PKA activation (Fig. 6A) and ERK1/2 phosphorylation (Fig. 6B) in HEK 293 cells transfected with both $\alpha 7$ nAChR and RIC3. Conversely, activation of PKA or ERK1/2 was not observed upon STII treatment when these cells were trans-

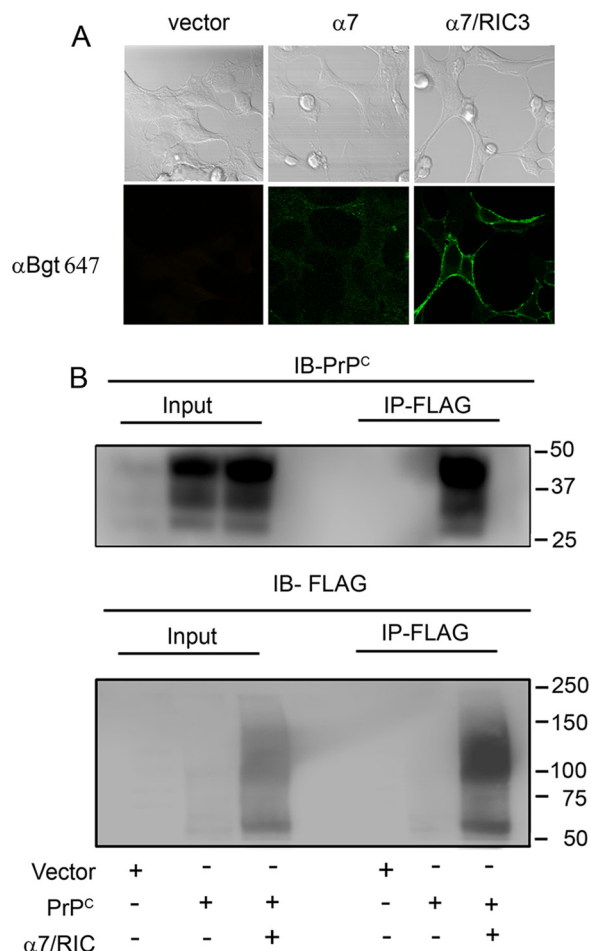


FIGURE 4. PrP^C interacts with $\alpha 7$ nAChR. *A*, HEK 293 cells were transfected with expression vector lacking insert (*vector*) or vectors encoding FLAG-tagged $\alpha 7$ nAChR ($\alpha 7$) or FLAG-tagged $\alpha 7$ nAChR and RIC3 ($\alpha 7/RIC3$). Cells were incubated with Alexa Fluor 647 αBgt and analyzed by confocal microscopy. Phase contrast images indicate the field of cells (*top panels*), and green fluorescence indicates Alexa Fluor 647 αBgt -labeled cells (*bottom panels*). *B*, HEK 293 cells were transfected with expression vector lacking insert (*Vector*) or expression vectors encoding PrP^C either alone (*PrP^C*) or co-transfected with FLAG-tagged $\alpha 7$ nAChR and RIC3 ($\alpha 7/RIC3$). Immunoprecipitation (*IP*) was performed with anti-FLAG antibodies, and proteins from total lysates (*Input*) or eluates (*IP-FLAG*) were immunoblotted (*IB*) with anti-PrP^C (*IB-PrP^C*) or anti-FLAG (*IB-FLAG*) antibodies.

fectured with empty vector or $\alpha 7$ nAChR alone (Fig. 6 and data not shown).

PrP^C-STI1 Interaction Induces Neuroprotection and Neuritogenesis through $\alpha 7$ nAChR—To determine whether STI1-PrP^C-mediated neuroprotection and neuritogenesis were also dependent on $\alpha 7$ nAChR, we analyzed activated caspase-3 levels and neurite outgrowth in hippocampal neurons. In primary neuronal cultures, staurosporine-induced cell death was blocked by STI1 treatment, and this was reversed by preincubation with αBgt (Fig. 7*A*). In addition, the treatment of hippocampal neurons with αBgt blocked PrP^C-STI1-mediated neuritogenesis, as measured by the percentage of cells with neurites (Fig. 7*B*) or the percentage of cells with neurite length >30 μm (Fig. 7*C*). Taken together, these data indicate that the PrP^C-STI1 interaction modulates $\alpha 7$ nAChR activity, thereby inducing Ca²⁺ influx and PKA and ERK1/2 activation and ultimately promoting neuronal protection and differentiation.

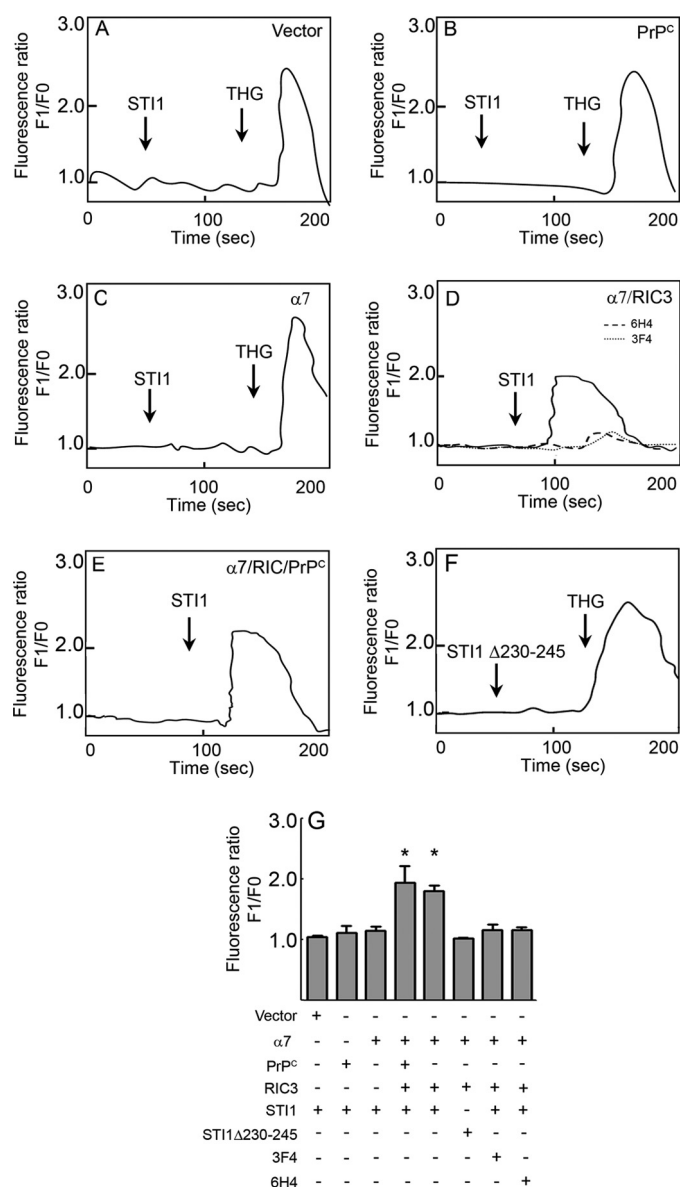


FIGURE 5. Expression of $\alpha 7$ nAChR rescues PrP^C-STI1-mediated Ca²⁺ influx in HEK 293 cells. *A–F*, HEK 293 cells were treated with 2 μM STI1 alone (*A–C* and *E*), STI1 in the presence of PrP^C antibodies 6H4 or 3F4 (*D*), or 2 μM STI1 deleted of the PrP^C binding site, STI1 $\Delta 230-245$ (*F*). Cells were transfected with empty vector (*n* = 5) (*A*), PrP^C (*n* = 4) (*B*), $\alpha 7$ nAChR (*n* = 4) (*C*), $\alpha 7$ nAChR and RIC3 (*D*) and treated with STI1 alone (*n* = 8) or in the presence of 6H4 (*n* = 4) or 3F4 (*n* = 3), PrP^C, $\alpha 7$ nAChR, and RIC3 (*n* = 4) (*E*) or $\alpha 7$ nAChR and RIC3 (*n* = 5) (*F*). Cells were treated with THG, when indicated, to test the level of intracellular Ca²⁺ stores. *G*, relative levels of intracellular Ca²⁺ in cells transfected and treated as indicated are shown. The results represent the mean \pm S.E. (*error bars*) of independent experiments compared by one-way ANOVA and Newman-Keuls post test. *, *p* < 0.01 compared with controls.

DISCUSSION

In this study, we demonstrate that PrP^C binding to STI1 increases Ca²⁺ influx in neurons through $\alpha 7$ nAChR. These results provide new insight into the physiological role of PrP^C as well as a novel mechanism by which PrP^C transduces extracellular signals.

The PrP^C-STI1 interaction has been shown to modulate neuronal differentiation and survival. Furthermore, these activities are dependent on activation of PKA, ERK1/2, and PI3K–mTOR via PrP^C (26, 27). STI1 is secreted from astrocytes (29), and its

$\alpha 7$ Nicotinic Acetylcholine Receptor Activation by PrP^C

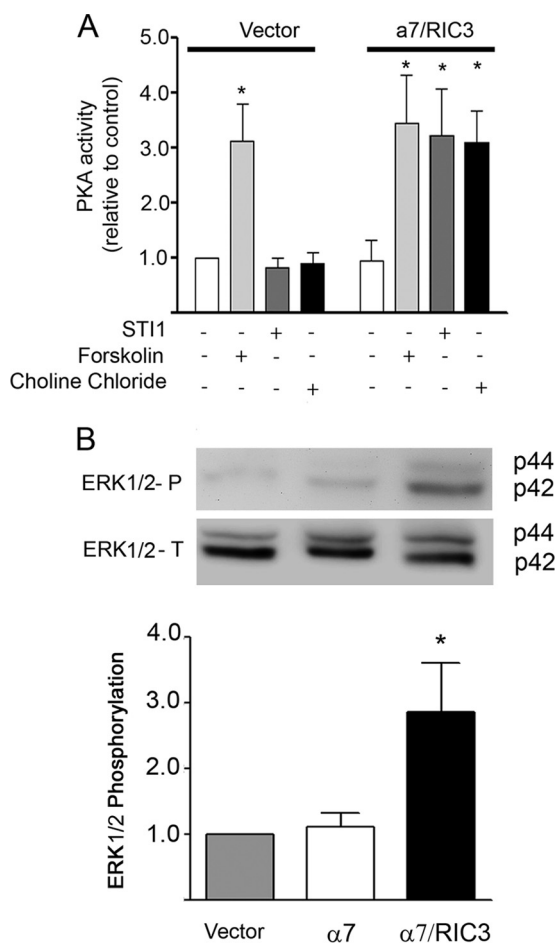


FIGURE 6. Expression of $\alpha 7$ nAChR in HEK 293 cells rescues PrP^C-STI1-induced PKA activity and ERK1/2 phosphorylation. PKA activity (A) and ERK1/2 phosphorylation (B) in HEK 293 cells transfected with empty vector or co-transfected with expression vectors for $\alpha 7$ nAChR and RIC3. Cells were treated with forskolin, STI1, or choline chloride as indicated. Relative levels of ERK1/2 activity represent the ratio between phosphorylated ERK1/2 and total ERK1/2 (upper panel) in cells treated with STI1 and normalized to cells transfected with empty vector. The results represent the mean \pm S.E. (error bars) of three independent experiments compared by one-way ANOVA and Newman-Keuls post test. *, $p < 0.01$ compared with controls.

activity is 100 times higher than recombinant STI1, probably due to a better folding or posttranslational modifications (28). The mechanisms associated with STI1 secretion are presently under investigation, but the protein is likely to use a nonconventional type of secretion due to the absence of a signal peptide (42). However, it is clear that secreted STI1 binds to PrP^C, potentially acting as a neurotrophic-like factor (25). Interestingly, hippocampal infusion of STI1 or an STI1-derived peptide (STI1pep230–245), which mimics the PrP^C binding site, increases PrP^C-dependent memory consolidation. On the other hand, antibodies against either STI1 or its peptide 230–245 were able to impair memory formation (43). These results indicate that the STI1-PrP^C interaction has physiological consequences *in vivo*.

PrP^C appears to act as a receptor or co-receptor for a number of ligands, including transmembrane, aggregated and soluble proteins. Therefore, it is important to dissect the mechanisms by which glycosylphosphatidylinositol-anchored PrP^C is able to transduce extracellular signals to the intracellular milieu. Pre-

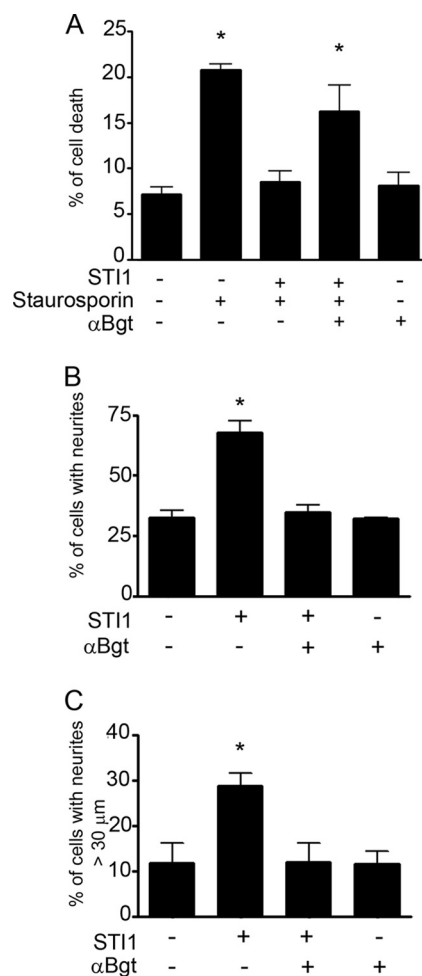


FIGURE 7. PrP^C-STI1 interaction promotes neuroprotection and neuritogenesis through $\alpha 7$ nAChR. A, PrP^C^{+/+} hippocampal neurons were treated with STI1 (30 min) or STI1 and α Bgt, followed by staurosporine, as indicated. Cells were immunolabeled with anti-activated caspase-3, which labels apoptotic cells. Data are represented as the percentage of activated caspase-3-positive cells. B and C, PrP^C^{+/+} hippocampal neurons were treated with STI1 alone, or STI1 plus α Bgt, as indicated, and neuritogenesis was measured as the percentage of cells with neurites or with neurites $> 30 \mu\text{m}$, respectively. The results represent the mean \pm S.E. (error bars) of three independent experiments, compared by one-way ANOVA and Newman-Keuls post test. *, $p < 0.01$ compared with controls.

viously, PrP^C has been shown to interact with neuronal cell adhesion molecule to stimulate Fyn-kinase (17). Furthermore, PrP^C has also been shown to associate with G protein-coupled serotonergic receptors, interfering with the intensities and/or dynamics of G protein activation by agonist-bound 5-HT receptors (18, 44). PrP^C also acts as a receptor for A β _{1–42} oligomers to inhibit synaptic plasticity in the form of long term potentiation (7). In addition, PrP^C interacts with the γ chain subunit of the extracellular matrix protein laminin (21). Our recent data demonstrate that laminin $\gamma 1$ chain interaction with PrP^C triggers neuronal signaling via group I metabotropic glutamate receptors, and regulates intracellular Ca²⁺ levels and neuritogenesis (62).

STI1 Activates $\alpha 7$ nAChR and Ca²⁺-dependent Signaling Pathways—Our data strongly indicate that STI1 activation of Ca²⁺ influx is dependent on its engagement with PrP^C, as neurons from PrP^C-null mice do not respond to STI1. Moreover, in

wild-type cultured hippocampal neurons, Ca²⁺ influx fails in the presence of STI1 lacking the PrP^C binding site.

The inhibition of STI1-evoked Ca²⁺ influx, ERK1/2 phosphorylation, and PKA activation in α Bgt-treated neurons is consistent with the fact that STI1 can modulate $\alpha 7$ nAChR via PrP^C. Moreover, the fact that STI1-mediated signaling is reconstituted in transfected HEK 293 cells supports the idea of a functional interaction between PrP^C and $\alpha 7$ nAChR. Indeed, we detected a physical interaction between PrP^C and $\alpha 7$ nAChR.

The mechanisms by which STI1 modulates $\alpha 7$ nAChR activity through its interaction with PrP^C are unknown. For instance, it is unclear whether STI1 and PrP^C act together to activate $\alpha 7$ nAChR, or whether they modulate $\alpha 7$ nAChR sensitivity to agonists. It should be noted that choline, a proposed $\alpha 7$ nAChR agonist (45), is normally found in the extracellular milieu, albeit at a concentration too low to activate $\alpha 7$ nAChR (45). Hence, it is possible that STI1-PrP^C engagement modulates the response of $\alpha 7$ nAChR to extracellular choline. Further experiments using electrophysiology techniques will be necessary to refine possible mechanisms.

Remarkably, the effects of STI1 on neurogenesis and protection against staurosporine-induced neuronal cell death were also completely blocked by α Bgt. Extensive studies have shown that $\alpha 7$ nAChR regulates many brain functions (45). These receptors are formed by homomeric assembly of five subunits and are preferentially permeable to Ca²⁺ (45). Furthermore, $\alpha 7$ nAChR activation has been shown to be neuroprotective (46–48) and to regulate learning and memory (for review, see Ref. 49) in an ERK1/2- and PKA-dependent manner (50).

The $\alpha 7$ nAChR has also been implicated in AD (51–54), as expression of these receptors is either decreased or increased in AD brains (55, 56) and animal models of AD (57). Furthermore, there is evidence that $\alpha 7$ nAChR interacts with A β _{1–42} oligomers (58, 59). Moreover, recent experiments involving $\alpha 7$ nAChR knock-out mice crossed with transgenic mice expressing mutated amyloid precursor protein suggest that the synaptic toxicity observed in the latter may be due in part to $\alpha 7$ nAChR (60). On the other hand, experiments using a separate transgenic mouse model for AD indicate that these receptors may be protective at early ages. Interestingly, drugs that prevent binding of A β _{1–42} to $\alpha 7$ nAChR seem to be beneficial in a model of AD (58). Hence, it seems that STI1 binding to PrP^C can hijack one of the key signaling pathways related to AD and learning and memory. Therefore, it is possible that STI1 modulation of a complex containing PrP^C and $\alpha 7$ nAChR may play an important role in AD.

Little is known regarding the role of nAChRs in prion diseases. Recent data demonstrated that PrP^C is co-localized with the $\beta 4$ subunit of nAChR in the brain and gastrointestinal tract. However, infection experiments using the Rocky Mountain Laboratory prion strain in $\beta 4$ nAChR knock-out mice demonstrated that these animals presented with the same disease incubation period when compared with controls (61).

In summary, we show that STI1 interaction with PrP^C can modulate Ca²⁺ influx via $\alpha 7$ nAChR, thereby promoting neuronal survival and differentiation (Fig. 8). Future experiments will need to define the mechanisms involved in PrP^C modulation of

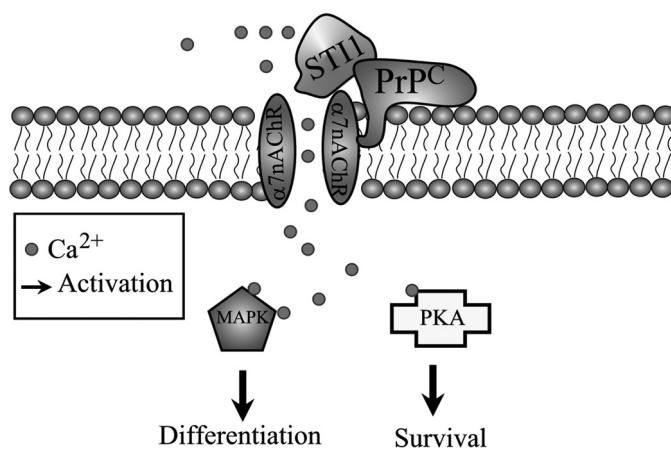


FIGURE 8. Schematic model of signaling events mediated by PrP^C-STI1 interaction. PrP^C-STI1 interaction modulates $\alpha 7$ nAChR, leading to Ca²⁺ influx and PKA and ERK1/2 activation. PKA and ERK1/2 activation promotes neuroprotection and neurogenesis, respectively.

$\alpha 7$ nAChR as well as the pathophysiological roles of this new signaling complex in prion diseases and AD.

REFERENCES

- Westergard, L., Christensen, H. M., and Harris, D. A. (2007) *Biochim. Biophys. Acta* **1772**, 629–644
- Linden, R., Martins, V. R., Prado, M. A., Cammarota, M., Izquierdo, I., and Brentani, R. R. (2008) *Physiol. Rev.* **88**, 673–728
- Linden, R., Martins, V. R., and Prado, M. A. (2009) Prion protein. UCSD-Nature Molecule Pages, 29 Jul 2009, doi:10.1038/mp.a003935.01
- Nimmrich, V., and Ebert, U. (2009) *Rev. Neurosci.* **20**, 1–12
- Walsh, D. M., and Selkoe, D. J. (2007) *J. Neurochem.* **101**, 1172–1184
- Klein, W. L. (2002) *Neurochem. Int.* **41**, 345–352
- Laurén, J., Gimbel, D. A., Nygaard, H. B., Gilbert, J. W., and Strittmatter, S. M. (2009) *Nature* **457**, 1128–1132
- Calella, A. M., Farinelli, M., Nuvolone, M., Mirante, O., Moos, R., Falsig, J., Mansuy, I. M., and Aguzzi, A. (2010) *EMBO Mol. Med.* **2**, 306–314
- Kessels, H. W., Nguyen, L. N., Nabavi, S., and Malinow, R. (2010) *Nature* **466**, E3–E4
- Parkin, E. T., Watt, N. T., Hussain, I., Eckman, E. A., Eckman, C. B., Manson, J. C., Baybutt, H. N., Turner, A. J., and Hooper, N. M. (2007) *Proc. Natl. Acad. Sci. U.S.A.* **104**, 11062–11067
- Cissé, M. A., Sunyach, C., Lefranc-Jullien, S., Postina, R., Vincent, B., and Checler, F. (2005) *J. Biol. Chem.* **280**, 40624–40631
- Guillot-Sestier, M. V., Sunyach, C., Druon, C., Scarzello, S., and Checler, F. (2009) *J. Biol. Chem.* **284**, 35973–35986
- Rieger, R., Edenhofer, F., Lasmézas, C. I., and Weiss, S. (1997) *Nat. Med.* **3**, 1383–1388
- Gauczynski, S., Peyrin, J. M., Haïk, S., Leucht, C., Hundt, C., Rieger, R., Krasemann, S., Deslys, J. P., Dormont, D., Lasmézas, C. I., and Weiss, S. (2001) *EMBO J.* **20**, 5863–5875
- Hundt, C., Peyrin, J. M., Haïk, S., Gauczynski, S., Leucht, C., Rieger, R., Riley, M. L., Deslys, J. P., Dormont, D., Lasmézas, C. I., and Weiss, S. (2001) *EMBO J.* **20**, 5876–5886
- Schmitt-Ulms, G., Legname, G., Baldwin, M. A., Ball, H. L., Bradon, N., Bosque, P. J., Crossin, K. L., Edelman, G. M., DeArmond, S. J., Cohen, F. E., and Prusiner, S. B. (2001) *J. Mol. Biol.* **314**, 1209–1225
- Santuccion, A., Sytnyk, V., Leshchyn'ska, I., and Schachner, M. (2005) *J. Cell Biol.* **169**, 341–354
- Mouillet-Richard, S., Pietri, M., Schneider, B., Vidal, C., Mutel, V., Launay, J. M., and Kellermann, O. (2005) *J. Biol. Chem.* **280**, 4592–4601
- Taylor, D. R., and Hooper, N. M. (2007) *Biochem. J.* **402**, 17–23
- Parkyn, C. J., Vermeulen, E. G., Mootoosamy, R. C., Sunyach, C., Jacobsen, C., Oxvig, C., Moestrup, S., Liu, Q., Bu, G., Jen, A., and Morris, R. J. (2008) *J. Cell Sci.* **121**, 773–783
- Graner, E., Mercadante, A. F., Zanata, S. M., Forlenza, O. V., Cabral, A. L.,

- Veiga, S. S., Juliano, M. A., Roesler, R., Walz, R., Minetti, A., Izquierdo, I., Martins, V. R., and Brentani, R. R. (2000) *Brain Res. Mol. Brain Res.* **76**, 85–92
22. Graner, E., Mercadante, A. F., Zanata, S. M., Martins, V. R., Jay, D. G., and Brentani, R. R. (2000) *FEBS Lett.* **482**, 257–260
23. Hajj, G. N., Lopes, M. H., Mercadante, A. F., Veiga, S. S., da Silveira, R. B., Santos, T. G., Ribeiro, K. C., Juliano, M. A., Jacchieri, S. G., Zanata, S. M., and Martins, V. R. (2007) *J. Cell Sci.* **120**, 1915–1926
24. Zanata, S. M., Lopes, M. H., Mercadante, A. F., Hajj, G. N., Chiarini, L. B., Nomizo, R., Freitas, A. R., Cabral, A. L., Lee, K. S., Juliano, M. A., de Oliveira, E., Jachieri, S. G., Burlingame, A., Huang, L., Linden, R., Brentani, R. R., and Martins, V. R. (2002) *EMBO J.* **21**, 3307–3316
25. Martins, V. R., Beraldo, F. H., Hajj, G. N., Lopes, M. H., Lee, K. S., Prado, M. M., and Linden, R. (2010) *Curr. Issues Mol. Biol.* **12**, 63–86
26. Lopes, M. H., Hajj, G. N., Muras, A. G., Mancini, G. L., Castro, R. M., Ribeiro, K. C., Brentani, R. R., Linden, R., and Martins, V. R. (2005) *J. Neurosci.* **25**, 11330–11339
27. Roffé, M., Beraldo, F. H., Bester, R., Nunziante, M., Bach, C., Mancini, G., Gilch, S., Vorberg, I., Castilho, B. A., Martins, V. R., and Hajj, G. N. (2010) *Proc. Natl. Acad. Sci. U.S.A.* **107**, 13147–13152
28. Caetano, F. A., Lopes, M. H., Hajj, G. N., Machado, C. F., Pinto, A. C., Magalhães, A. C., Vieira, M. P., Américo, T. A., Massensini, A. R., Priola, S. A., Vorberg, I., Gomez, M. V., Linden, R., Prado, V. F., Martins, V. R., and Prado, M. A. (2008) *J. Neurosci.* **28**, 6691–6702
29. Lima, F. R., Arantes, C. P., Muras, A. G., Nomizo, R., Brentani, R. R., and Martins, V. R. (2007) *J. Neurochem.* **103**, 2164–2176
30. Cullen, B. R. (1987) *Methods Enzymol.* **152**, 684–704
31. Dale, L. B., Bhattacharya, M., Anborgh, P. H., Murdoch, B., Bhatia, M., Nakanishi, S., and Ferguson, S. S. (2000) *J. Biol. Chem.* **275**, 38213–38220
32. Cooper, D. M., Mons, N., and Karpen, J. W. (1995) *Nature* **374**, 421–424
33. Fierro, A. F., Wurth, G. A., and Zweifach, A. (2004) *J. Biol. Chem.* **279**, 25646–25652
34. Brini, M., Míuzzo, M., Pierobon, N., Negro, A., and Sorgato, M. C. (2005) *Mol. Biol. Cell* **16**, 2799–2808
35. Korte, S., Vassallo, N., Kramer, M. L., Kretzschmar, H. A., and Herms, J. (2003) *J. Neurochem.* **87**, 1037–1042
36. Whatley, S. A., Powell, J. F., Politopoulou, G., Campbell, I. C., Brammer, M. J., and Percy, N. S. (1995) *Neuroreport* **6**, 2333–2337
37. Bitner, R. S., Bunnelle, W. H., Anderson, D. J., Briggs, C. A., Buccafusco, J., Curzon, P., Decker, M. W., Frost, J. M., Gronlien, J. H., Gubbins, E., Li, J., Malysz, J., Markosyan, S., Marsh, K., Meyer, M. D., Nikkel, A. L., Radek, R. J., Robb, H. M., Timmermann, D., Sullivan, J. P., and Gopalakrishnan, M. (2007) *J. Neurosci.* **27**, 10578–10587
38. Broide, R. S., and Leslie, F. M. (1999) *Mol. Neurobiol.* **20**, 1–16
39. Shimohama, S., Greenwald, D. L., Shafro, D. H., Akaika, A., Maeda, T., Kaneko, S., Kimura, J., Simpkins, C. E., Day, A. L., and Meyer, E. M. (1998) *Brain Res.* **779**, 359–363
40. Jonnal, R. R., and Buccafusco, J. J. (2001) *J. Neurosci. Res.* **66**, 565–572
41. Williams, M. E., Burton, B., Urrutia, A., Shcherbatko, A., Chavez-Noriega, L. E., Cohen, C. J., and Aiyar, J. (2005) *J. Biol. Chem.* **280**, 1257–1263
42. Keller, M., Rüegg, A., Werner, S., and Beer, H. D. (2008) *Cell* **132**, 818–831
43. Coitinho, A. S., Lopes, M. H., Hajj, G. N., Rossato, J. I., Freitas, A. R., Castro, C. C., Cammarota, M., Brentani, R. R., Izquierdo, I., and Martins, V. R. (2007) *Neurobiol. Dis.* **26**, 282–290
44. Mouillet-Richard, S., Schneider, B., Pradines, E., Pietri, M., Ermonval, M., Grassi, J., Richards, J. G., Mutel, V., Launay, J. M., and Kellermann, O. (2007) *Ann. N.Y. Acad. Sci.* **1096**, 106–119
45. Albuquerque, E. X., Pereira, E. F., Alkondon, M., and Rogers, S. W. (2009) *Physiol. Rev.* **89**, 73–120
46. Dajas-Bailador, F., and Wonnacott, S. (2004) *Trends Pharmacol. Sci.* **25**, 317–324
47. Akaike, A., Takada-Takatori, Y., Kume, T., and Izumi, Y. (2010) *J. Mol. Neurosci.* **40**, 211–216
48. Dajas-Bailador, F. A., Lima, P. A., and Wonnacott, S. (2000) *Neuropharmacology* **39**, 2799–2807
49. Thomsen, M. S., Hansen, H. H., Timmerman, D. B., and Mikkelsen, J. D. (2010) *Curr. Pharm. Des.* **16**, 323–343
50. Dajas-Bailador, F. A., Soliakov, L., and Wonnacott, S. (2002) *J. Neurochem.* **80**, 520–530
51. Hernandez, C. M., Kayed, R., Zheng, H., Sweatt, J. D., and Dineley, K. T. (2010) *J. Neurosci.* **30**, 2442–2453
52. Ren, K., King, M. A., Liu, J., Siemann, J., Altman, M., Meyers, C., Hughes, J. A., and Meyer, E. M. (2007) *Neuroscience* **148**, 230–237
53. Kihara, T., Shimohama, S., Sawada, H., Honda, K., Nakamizo, T., Shibasaki, H., Kume, T., and Akaike, A. (2001) *J. Biol. Chem.* **276**, 13541–13546
54. Buckingham, S. D., Jones, A. K., Brown, L. A., and Sattelle, D. B. (2009) *Pharmacol. Rev.* **61**, 39–61
55. Jones, I. W., Westmacott, A., Chan, E., Jones, R. W., Dineley, K., O'Neill, M. J., and Wonnacott, S. (2006) *J. Mol. Neurosci.* **30**, 83–84
56. Teaktong, T., Graham, A. J., Court JA, Perry, R. H., Jaros, E., Johnson, M., Hall, R., and Perry, E. K. (2004) *J. Neurol. Sci.* **225**, 39–49
57. Dineley, K. T., Xia, X., Bui, D., Sweatt, J. D., and Zheng, H. (2002) *J. Biol. Chem.* **277**, 22768–22780
58. Wang, H. Y., Stucky, A., Liu, J., Shen, C., Trocme-Thibierge, C., and Morain, P. (2009) *J. Neurosci.* **29**, 10961–10973
59. Wang, H. Y., Lee, D. H., D'Andrea, M. R., Peterson, P. A., Shank, R. P., and Reitz, A. B. (2000) *J. Biol. Chem.* **275**, 5626–5632
60. Dziewczapolski, G., Glogowski, C. M., Masliah, E., and Heinemann, S. F. (2009) *J. Neurosci.* **29**, 8805–8815
61. Petrakis, S., Irinopoulou, T., Panagiotidis, C. H., Engelstein, R., Lindstrom, J., Orr-Urtreger, A., Gabizon, R., Grigoriadis, N., and Sklaviadis, T. (2008) *Eur. J. Neurosci.* **27**, 612–620
62. Beraldo, F. H., Arantes, C. P., Santos, T. G., Machado, C. F., Roffe, M., Hajj, G. N., Lee, K. S., Magalhães, A. C., Caetano, F. A., Mancini, G. L., Lopes, M. H., Américo, T. A., Magdesian, M. H., Ferguson, S. S., Linden, R., Prado, M. A., and Martins, V. R. (2010) *FASEB J.*, in press